J Neuropathol Exp Neurol
Vol. 68, No. 12
December 2009
pp. 1326–1338

ORIGINAL ARTICLE

bcl-2/Adenovirus E1B 19-kd Interacting Protein 3 (BNIP3) Regulates Hypoxia-Induced Neural Precursor Cell Death

K.C. Walls, PhD, Arindam P. Ghosh, MD, Mary E. Ballestas, PhD,
Barbara J. Klocke, MS, and Kevin A. Roth, MD, PhD

Abstract

Perinatal hypoxia-ischemia may result in long-term neurological deficits. In addition to producing neuron death, HI causes death of neural precursor cells (NPCs) in the developing brain. To characterize the molecular pathways that regulate hypoxia-induced death of NPCs, we treated a mouse neural stem cell line (C17.2 cells) and fibroblastic growth factor II–expanded primary NPCs derived from wild-type or gene-disrupted mice, with oxygen glucose deprivation or the hypoxia mimetics desferrioxamine or cobalt chloride. Neural precursor cells undergoing hypoxia exhibited time- and concentration-dependent caspase-3 activation and cell death, which was significantly reduced by treatment with a broad caspase inhibitor or protein synthesis inhibition. Bax/Bak-deficient NPCs were protected from desferrioxamine-induced death and exhibited minimal caspase-3 activation. Oxygen glucose deprivation or hypoxia-mimetic exposure also resulted in increased hypoxia-inducible factor α and bcl-2/adenovirus E1B 19-kd interacting protein 3 (BNIP3) expression. BNIP3 shRNA treatment failed to affect hypoxia-induced caspase-3 activation but inhibited cell death and nuclear translocation of apoptosis-inducing factor, indicating that BNIP3 is an important regulator of caspase-independent NPC death after hypoxia. These studies demonstrate that hypoxia activates both caspase-dependent and -independent NPC death pathways that are critically regulated by multiple Bcl-2 family members.

Key Words: Apoptosis, Apoptosis-inducing factor, BNIP3, Hypoxia.

INTRODUCTION

Programmed cell death of neural precursor cells (NPCs) is important for normal nervous system development, but pathological apoptosis of NPCs under conditions such as perinatal hypoxia-ischemia (HI) may contribute to long-term neurological dysfunction (1). Hypoxia induces a stimulus-specific cell death response resulting in the stabilization of hypoxia-inducible factor (HIF) and p53 (2). During normoxia, proline hydroxylase domain proteins hydroxylate HIF-1α, which is required for its binding to von Hippel-Lindau tumor suppressor protein, a component of an E3 ubiquitin ligase, thus resulting in HIF-1α proteosomal degradation (3–5). During hypoxia, HIF-1α remains non-hydroxylated, which leads to its stabilization and transactivation of target genes through hypoxia-regulated elements, which may result in either apoptotic or non-apoptotic cell death (6–8). Hypoxia mimetics, such as desferrioxamine (DFO) and cobalt chloride ($CoCl_2$), sequester iron and ascorbate, the rate-limiting molecules needed by prolylhydroxylases, thus effectively inhibiting HIF-1α proteosomal degradation, leading to HIF-1α and HIF-β dimerization and the induction of HIF-inducible genes (9, 10).

Programmed cell death has been classified as type I (apoptotic) or type II (autophagic) and is important for normal nervous system development (11, 12). Apoptosis is mediated by Bcl-2 family protein members. Bcl-2 prosurvival proteins negatively regulate proapoptotic proteins Bax and Bak via interactions between their Bcl-2 homology (BH) domains. The interaction between Bcl-2 and Bax may be inhibited by BH3-only proapoptotic proteins in a stimulus-specific pattern. bcl-2/adenovirus E1B 19-kd interacting protein 3 (BNIP3), a BH3-only protein, has been previously implicated in hypoxia-induced cell death (13, 14). The promoter of BNIP3 contains a functional hypoxia response element and is activated by E2F and HIF-1α under hypoxic conditions and by stimuli such as cyanide, ceramide, and arsenic trioxide (15–17). BNIP3 and other Bcl-2 family members also regulate autophagy, a naturally occurring catabolic process that sequesters and degrades cytosolic contents via the lysosome (18). The Bcl-2 and BNIP3 interaction increases during hypoxia, whereas the Beclin1 and Bcl-2 interaction decreases, thus promoting the accumulation of autophagic vacuoles (19).

To investigate the molecular mechanisms regulating hypoxia-induced NPC death, we used the hypoxia mimetics DFO and $CoCl_2$ and oxygen glucose deprivation (OGD) and found that these agents increased expression of HIF-1α and BNIP3. Hypoxia-induced NPC death occurred through both a Bax/Bak-mediated caspase-dependent pathway and a caspase-independent pathway that is regulated by BNIP3.

From the Departments of Pathology (KCW, APG, BJK, KAR), Cell Biology (KCW), Genetics (APG), and Pediatrics and Infectious Disease (MEB), University of Alabama at Birmingham, Birmingham, Alabama.
Send correspondence and reprint requests to: Kevin A. Roth, MD, PhD, Department of Pathology, University of Alabama at Birmingham, Birmingham AL 35294-0017; E-mail: karoth@uab.edu; kcwalls@uab.edu
This work was supported by grants from the National Institutes of Health (NS35107 and NS41962) and UAB Core Facilities (NS47466 and NS57098).
The C17.2 cell line was generously provided by Dr Evan Snyder (Burnham Institute).

MATERIALS AND METHODS

Animals

C57BL/6J mice were used in all experiments. Mice were housed and cared for according to the National Institutes of Health's *Guide for the Care and Use of Laboratory Animals*. All animal protocols were approved by the Institutional Animal Care and Use Committee of the University of Alabama at Birmingham. The generation of Bax-deficient mice has been described previously (20). The genotypes for gene-disrupted mice were determined from tail DNA extracts by polymerase chain reaction (PCR).

Cell Culture

Fibroblast growth factor 2 (FGF2) has been previously demonstrated to stimulate NPC proliferation while maintaining their undifferentiated state. Neural precursor cell cultures were established from the cerebellum of postnatal days 6 to 7 male and female mice as previously published (21). Briefly, freshly isolated, dissociated cerebellar cells were incubated at 37°C in humidified 5% CO_2/95% air atmosphere; this allowed glia and postmitotic neurons to adhere, whereas nonadherent cell populations were suspended in the supernatant. After 24 hours, nonadherent cells in the supernatant were transferred to a poly-L-lysine–coated (Sigma, St Louis, MO) and laminin-coated (BD Bioscience, Bedford, MA) flask. Neural precursor cells formed an adherent monolayer and were grown until they were 70% confluent. Fresh FGF2-containing media was added every 3 to 4 days. Cells were passaged and plated as previously described (21). A small aliquot of cells was stained with trypan blue and counted. Thirty thousand cells were plated per well and allowed to grow for 2 to 4 days in FGF2-containing media. Experimental agents (DFO, $CoCl_2$) were added directly to the medium.

C17.2 Cells

The C17.2 neural stem cell line was a generous gift from Dr Evan Y. Snyder (Burnham Institute, La Jolla, CA). C17.2 cells were derived from the mouse cerebellar external granule cell layer and possess neural stem cell properties (22). C17.2 cells were cultured in highly modified Dulbecco's modified Eagle medium (Gibco, Grand Island, NY) containing 1% penicillin/streptomycin, 1% L-glutamine (Sigma), 5% horse serum, and 10% fetal calf serum (Gibco). The cells were passaged every other day by trypsinization and adding a 10th of the cells to a new T75 flask. Cells were plated on 48-well plates at a density of 30,000 cells per well. Cultures were incubated for 1 day before treatment. Desferrioxamine, $CoCl_2$, and boc-asp-FMK (50 μmol/L) were added to 3% horse and fetal calf sera–containing media to keep C17.2 cells in a proliferative state. For OGD studies, cells were cultured in Dulbecco's modified Eagle medium without (−) glucose placed in either a standard incubator (normoxia) or into a hypoxia chamber in which the oxygen concentration is maintained below 1%.

Cell Viability and Caspase Assays

Cell viability was assessed by the Calcein AM assay (Molecular Probes, Eugene, OR). Briefly, cells were washed in Locke buffer (in mmol/L: NaCl, 154; KCl, 5.6; $NaHCO_3$, 3.6; $CaCl_2$, 2.3; $MgCl_2$, 1.2; glucose, 5.6; and HEPES, 5; pH 7.4). Calcein AM, 5 μM, was diluted in this buffer and added to cells; they were then incubated at 37°C for 30 minutes. Calcein AM conversion was measured using a fluorescence plate reader (excitation, 488 nm; emission, 530 nM). To calculate the percentage of dead cells after DFO exposure, live and dead cell numbers were determined by using Calcein AM and propidium iodide. To assess caspase activity in vitro, we used the Asp-Glu-Val-Asp 7-amino-4-methylcoumarin (DEVD-AMC)-labeled caspase substrate cleavage assay (Biomol, Plymouth Meeting, PA). After treatment, cells were lysed in 100 μL buffer A (10 mmol/L HEPES, pH 7.4; 42 mmol/L KCl; 5 mmol/L $MgCl_2$; 1 mmol/L dithiothreitol [DTT]; 0.5% CHAPS; 10% sucrose; 1 mmol/L phenylmethylsulfonyl; and 1 μg/mL leupeptin) followed by 150 μL of buffer B (25 mmol/L HEPES, pH 7.4; 1 mmol/L EDTA; 0.1% CHAPS; 10% sucrose; and 3 mmol/L DTT) containing 10 μmol/L DEVD-AMC and incubated at 37°C for 30 minutes. Production of the fluorescent AMC caspase-3 product was measured with a fluorescence plate reader (excitation, 360 nM; emission, 460 nM). Both assays were expressed in comparison to untreated controls.

Immunocytochemistry

Neural precursor cell cultures were fixed in 4% paraformaldehyde for 20 minutes at 4°C followed by phosphate-buffered saline (PBS) wash and stored at 4°C. Cells were permeabilized with PBS-blocking buffer (PBS with 0.1% bovine serum albumin, 0.3% Triton X-100, and 0.2% nonfat powdered milk) for 30 minutes at room temperature. Primary antibodies were incubated overnight at 4°C in PBS-blocking buffer without Triton. The primary antibodies used were rabbit anti-LC3, cleaved caspase-3 (9661), pyruvate dehydrogenase (PDH; 3205), and BNIP3 (3769) (all from Cell Signaling Technologies, Danvers, MA), and goat anti-apoptosis-inducing factor (AIF) (sc-9416; Santa Cruz Biotechnology, Santa Cruz, CA). Plates were washed with PBS, and secondary antibody was applied, either horseradish peroxidase-conjugated horse anti-rabbit SuperPicture (Zymed Laboratories Inc, South San Francisco, CA) or anti-goat Vector Impress (Vector Laboratories, Burlingame, CA) for 1 hour at room temperature. Plates were washed with PBS, and immunoreactivity was detected using Tyramide Signal Amplification system (Perkin-Elmer Life Science Products, Boston, MA). After washing with PBS, the cells were counterstained with bisbenzimide (2 μg/mL; Hoechst 33258; Sigma). Plates were examined using a Zeiss Axioskop microscope equipped with epifluorescence. Images were captured using Axiovision software (ZEISS Microscopy & Imaging, Jena, Germany).

Confocal Laser Scanning Microscopy

For dual labeling of BNIP3 and PDH, immunocytochemical analysis was performed as described above. After Tyramide Signal Amplification detection of BNIP3, 0.3% H_2O_2 was added for 10 minutes to destroy any residual horseradish

peroxidase activity followed by washing with PBS. Cells were then incubated for 30 minutes in PBS-blocking buffer containing Triton followed by diluted PDH in PBS-blocking buffer without Triton overnight. The next day, goat anti-mouse Vector Impress (Vector Laboratories) was applied for 1 hour followed by Tyramide Signal Amplification detection (Perkin-Elmer Life Science Products). Cells were then stained with bisbenzimide; coverslips were placed, and images were taken of the cells using a Leica Confocal TCS SP1 UV unit (Leica Microsystems, Mannheim, Germany) with a Coherent Laser Group Enterprise UV laser for blue fluorochromes, argon laser for green fluorochromes, and helium/neon laser for far-red fluorochromes. Filter sets for fluorescein and Cy3 were used (Chroma Technology Corp, Brattleboro, VT). Fluorochrome excitation and emission were controlled by using an acousto-optic tunable filter and prism spectrophotometer. The 100× objective and Leica confocal software were used to acquire images from untreated and DFO-treated neural stem cells.

RNA Extraction and Reverse Transcriptase–Polymerase Chain Reaction

After DFO treatment, NPCs were trypsinized as described above. Suspensions were centrifuged at 1,700 revolutions per minute, and the cells were then lysed using Trizol reagent (Invitrogen, Carlsbad, CA), and RNA was extracted by following the manufacturer's protocol. RNA (1 μg) was incubated with 200-ng random hexamers, 0.5 mmol/L deoxyribonucleotide triphosphate, and RNase-free water at 65°C for 10 minutes (Invitrogen). After incubation, 5× first-strand buffer, 5 mmol/L DTT, 40 U RNAseOUT, and 200 U SuperScript III (Invitrogen, Carlsbad, CA) were added, and the reaction mixture was incubated at room temperature for

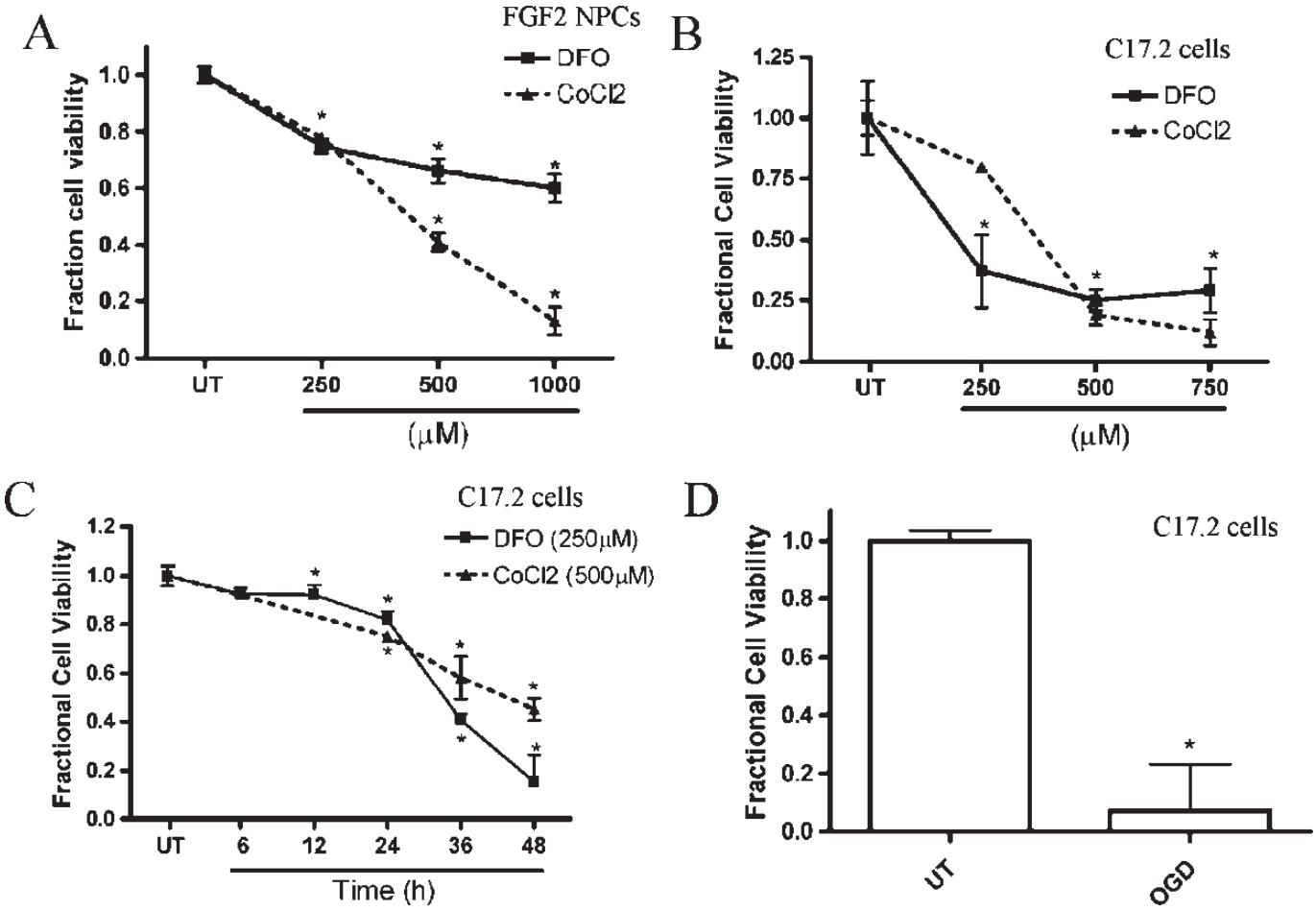

FIGURE 1. Hypoxia mimetics and oxygen glucose deprivation (OGD) cause concentration- and time-dependent decreases in neural precursor cell (NPC) viability. **(A)** NPC viability decreased significantly after cobalt chloride ($CoCl_2$) and desferrioxamine (DFO) treatment at concentrations greater than or equal to 250 μmol/L for 36 hours compared with untreated (UT) cells. Viability was assessed by measuring the fluorescence produced from the cleavage of Calcein AM by intracellular esterases in intact cells. **(B)** C17.2 cell viability decreased significantly after 36 hours' exposure to DFO and $CoCl_2$ at concentrations greater than or equal to 250 μmol/L for 36 hours compared with UT cells. **(C)** C17.2 cells exposed to 250 μmol/L DFO or 500 μmol/L $CoCl_2$ exhibited decreased cell viability by 24 hours, which further decreased at 48 hours. **(D)** C17.2 cells subjected to 16-hour OGD resulted in decreased cell viability. Data points represent mean ± SEM, with n = 6. *, $p < 0.01$ by 1-way analysis of variance/Bonferroni post hoc test versus UT controls. FGF2, fibroblast growth factor 2.

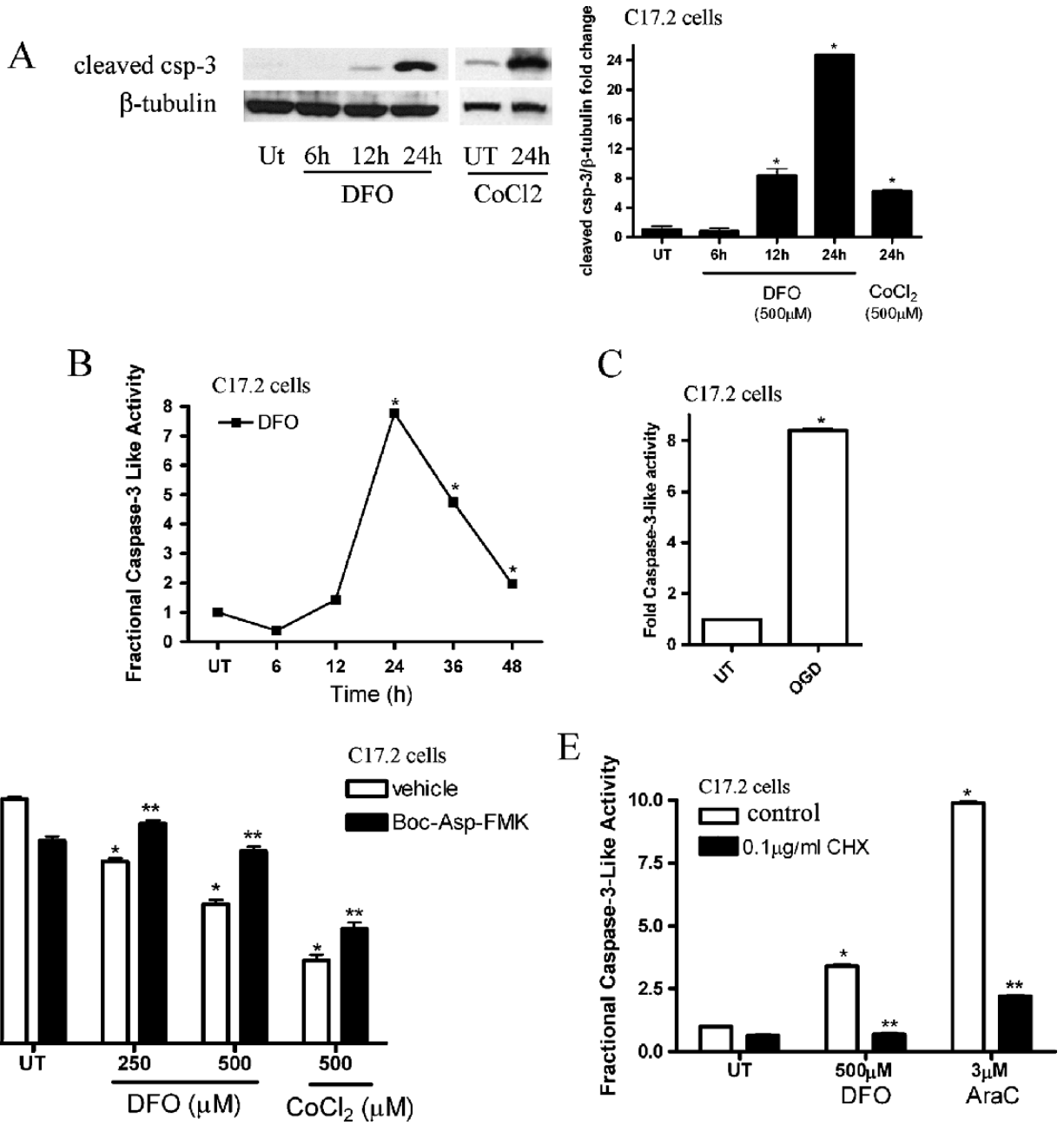

FIGURE 2. Hypoxia causes neural precursor cell caspase-3 activation. **(A)** Biochemical detection of cleaved caspase-3 revealed a significant increase at 12 to 24 hours after 250 μmol/L desferrioxamine (DFO) exposure or 500 μmol/L cobalt chloride ($CoCl_2$) in C17.2 cells (24 hours) compared with untreated (UT) cells and at 6 hours' time point. Western blots were digitized by UN-SCAN-IT software, and cleaved caspase-3/β-tubulin pixel totals were determined, normalized to UT groups, and values were expressed as fold change. The data represent mean ± SEM, with n = 4. *, $p < 0.01$ by 2-way analysis of variance (ANOVA)/Bonferroni post hoc test versus UT. **(B)** DFO (250 μmol/L) treatment for 12 to 48 hours leads to a significant increase in caspase-3 enzymatic activity as measured by the fluorescence produced by DEVD-AMC cleavage. Data points represent mean ± SEM, with n = 6. *, $p < 0.01$ by 1-way ANOVA/Bonferroni post hoc test versus UT controls. **(C)** Oxygen glucose deprivation exposure for 12 hours caused a significant increase in casapse-3–like activity in C17.2 cells relative to UT cells. Data points represent mean ± SEM, with n = 6. *, $p < 0.01$ by 1-way ANOVA/Bonferroni post hoc test versus UT controls. **(D)** Coincubation with boc-asp-FMK (40 μmol/L), a broad caspase inhibitor, attenuates DFO- and $CoCl_2$-induced cell death after 24-hour treatment. *, $p < 0.01$ by 2-way ANOVA/Bonferroni post hoc test versus matched treated group. **(E)** Cycloheximide, a protein synthesis inhibitor, significantly attenuated caspase-3–like activation after 12-hour DFO (500 μmol/L) or cytosine arabinoside (AraC) (3μmol/L) exposure. *, $p < 0.01$ by 2-way ANOVA/Bonferroni posttest versus treated in the presence of cycloheximide (CHX).

5 minutes, at 50°C for 60 minutes, at 70°C for 15 minutes, and at 4°C for 10 minutes. Cyclophilin was used as a cDNA control. Semiquantitative reverse transcriptase (RT)–PCR was performed using Taq DNA polymerase (Sigma) according to manufacturer's instructions, and the following primers were used: HIF-α forward primer: TGAGGCTCACCATCA GTTAT, HIF-1α reverse primer: CCTCATGGTCACATGG ATGA, BNIP3 forward primer: CCCTGCTACCTCTCGG TGAC, BNIP3 reverse primer: GCTGGGCATCCAACAGT ATT, cyclophilin forward primer: CAAGACTGAGTGGCT GGATGG, cyclophilin reverse primer: TAAAATGCCCGC AAGTCAAAGAAA. Polymerase chain reaction products were run on 1.5% agarose gels and stained with ethidium bromide and photoimaged with a UV transilluminator.

RNA Interference

Lentiviral shRNA (BNIP3) constructs were purchased from Open Biosystems (RMM4534_001478188). Plasmids containing the shRNAs were cotransfected into 293FT cells together with packaging plasmids, by following the manufacturer's protocol (ViraPower Lentiviral Expression Systems kit; Invitrogen). C17.2 cells were passaged and plated in a 6-well plate and allowed to adhere for 24 hours before infection. C17.2 cells were subjected to lentiviral infection in the presence of polybrene overnight, and media was replaced by fresh media on the following day. After 24 hours, cells were selected by treating with media containing 1.5 μg/ml puromycin. Protein levels and experiments were assessed after at least 72 hours, and cells were passaged as needed.

Lysate Preparation

Preparation of whole cell lysates was performed as follows. Briefly, cells were suspended in lysis buffer (2 mmol/L Tris-HCl, 150 mmol/L NaCl, 2 mmol/L EDTA, 1% Triton X-100, and 10% glycerol) with 1% phenylmethylsulfonyl, 1% protease inhibitor cocktail (Sigma), and 1% phosphatase inhibitor cocktail protease and incubated on ice for 30 minutes with vortexing every 10 minutes. Samples were centrifuged at 13,000 × *g* for 15 minutes, and protein concentrations determined using a Pierce BCA kit (Pierce, Rockford, IL).

Preparation of nuclear and cytoplasmic fractions was performed using the NE-PER Biotechnology kit (Pierce) according to the manufacturer's instructions. Briefly, cells were suspended in reagent I (Cer I) containing 1% protease inhibitor cocktail (Sigma) and 1% phosphatase inhibitor cocktail (Sigma) and then incubated on ice for 10 minutes; 11 μl of reagent II (Cer II) was added to the mixture, vortexed, and then incubated on ice for 1 minute. The sample was

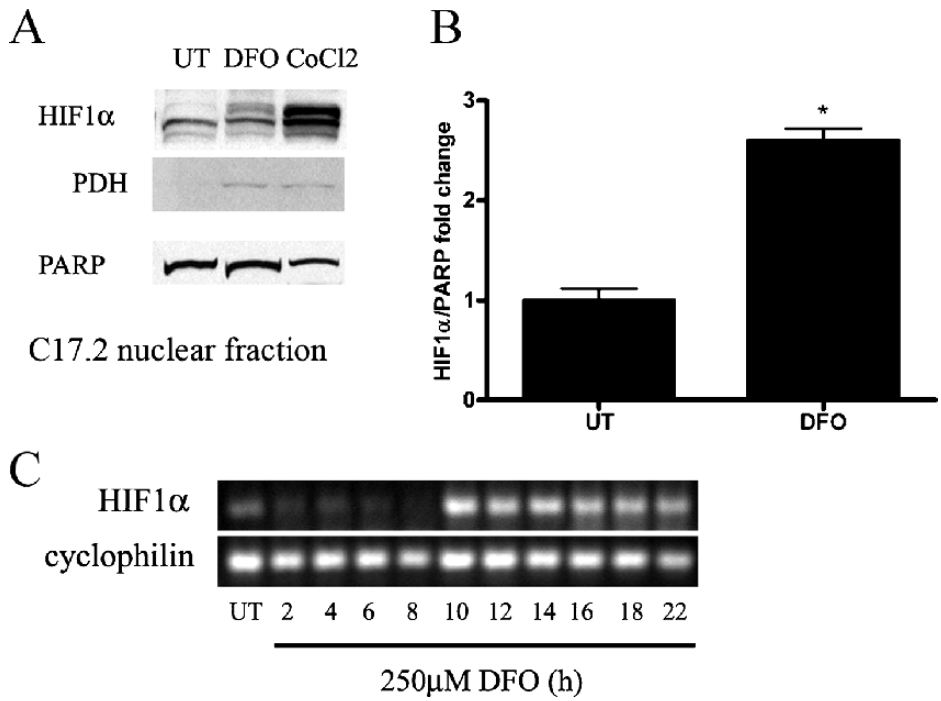

FIGURE 3. Hypoxic stimuli induce hypoxia-inducible factor 1α (HIF-1α) expression. **(A)** Western blot analysis was performed on nuclear fractions prepared from C17.2 cells treated with 250 μmol/L desferrioxamine (DFO) or 500 μmol/L cobalt chloride ($CoCl_2$) for 24 hours. DFO- and $CoCl_2$-treated neural precursor cell had increased HIF-1α protein levels compared with untreated (UT) cells. **(B)** Western blots for panel **A** were digitized by UN-SCAN-IT software, and averages for HIF-1α/poly(ADP-ribose) polymerase (PARP) pixel totals were calculated and the data points expressed in fold change. Data points in **A** represent mean ± SEM, with n = 4. *, $p < 0.01$ by 1-way analysis of variance/Bonferroni post hoc test versus UT controls. **(C)** DFO-induced an increase in HIF-1α expression after 10 hours that persisted for at least an additional 10 hours compared with UT cells and 2- to 8-hour time points. Cyclophilin was used as a cDNA loading control. PDH, pyruvate dehydrogenase.

centrifuged at maximum speed (13,000 × *g*) for 10 minutes at 4°C. The supernatant (cytoplasmic fraction) was transferred to a new tube and stored at −80°C. The pellet was resuspended in 100 μL of ice-cold nuclear extraction reagent and vortexed for 15 seconds every 10 minutes over a total of 40 minutes. The sample was then centrifuged at maximum speed (13,000 × *g*) for 10 minutes at 4°C. The supernatant (nuclear fraction) was transferred to a new tube and stored at −80°C. Protein concentrations were determined as above.

Western Blot

Equal amounts of whole cell lysates were resolved by sodium dodecyl sulfate–polyacrylamide gel electrophoresis and transferred to polyvinylidene fluoride. Blots were blocked for 1 hour at room temperature, 5% milk in wash buffer (200 mmol/L Tris base, 1.37 mol/L NaCl, 1% Tween 20; pH 7.6), followed by overnight incubation with primary antibodies. Blots transferred and probed for either AIF (4642), BNIP3 (3769), poly(ADP-ribose) polymerase (PARP) (9542), cleaved caspase-3 (9661) (all from Cell Signaling Technologies), HIF 1α (400080; Calbiochem/EMD, Gibbstown, NJ), or β-tubulin (sc-9104) (Santa Cruz Biotechnology) served as a loading control. After primary antibody incubation, blots were washed with 1× TBS containing 0.1% Tween 20, then incubated with secondary antibody, either goat anti-rabbit IgG (BioRad, Hercules, CA) or anti-mouse IgG (Cell Signaling Technologies), for 1 hour at room temperature and washed. Signal was detected using Supersignal chemiluminescence (Pierce) or ECL (Amersham, Fairfield, CT). Western blots were scanned into Adobe Photoshop and digitized using the UN-SCAN-IT software, version 6.1 (UN-SCAN-IT, Orem, UT).

Statistics

For experiments involving quantification, SEMs were determined from at least 3 independent experiments with an n of 1 representing 1 gene-disrupted mouse accompanied by 1 wild-type littermate control or separate experiments from different C17.2 passages. The effects of genotype for each age were analyzed for significance using a 2-way analysis of variance, followed by Bonferroni test for all pairwise comparisons. In all cases, a $p \leq 0.05$ was considered significant.

RESULTS

Hypoxia Causes Time-Dependent Neural Precursor Cell Death

To dissect the molecular pathways associated with hypoxia-induced death of NPCs, we used mitogenically expanded mouse NPCs and C17.2 cells, a mouse neural stem cell line. We developed an in vitro hypoxia model by treating these cells with the iron chelator DFO or $CoCl_2$. Both NPCs and C17.2 cells exposed to DFO or $CoCl_2$ exhibited concentration- and time-dependent decreases in viability (Figs. 1A–C, and data not shown). Oxygen glucose deprivation has been previously used to model the effects of HI on neuronal cells in vitro (23). C17.2 cells exposed to OGD for 16 hours showed significantly decreased cell viability compared with untreated cells (Fig. 1D).

Caspase Activation in Hypoxia-Induced Neural Precursor Cell Death

We previously demonstrated that C17.2 neural stem cells and NPCs undergo cell death in response to staurosporine treatment or genotoxic insult (21). To examine the apoptotic signaling cascade involved in hypoxia-induced NPC death, we measured caspase-3 activation, an important component of the apoptotic death pathway. To detect caspase-3 activation, we performed Western blot analysis for the cleaved activated form of caspase-3 on whole cell lysates obtained from C17.2 cells treated in the absence or presence of 250 μmol/L DFO from 6 to 24 hours or 500 μmol/L $CoCl_2$ for 24 hours. Whole cell lysates from C17.2 cells

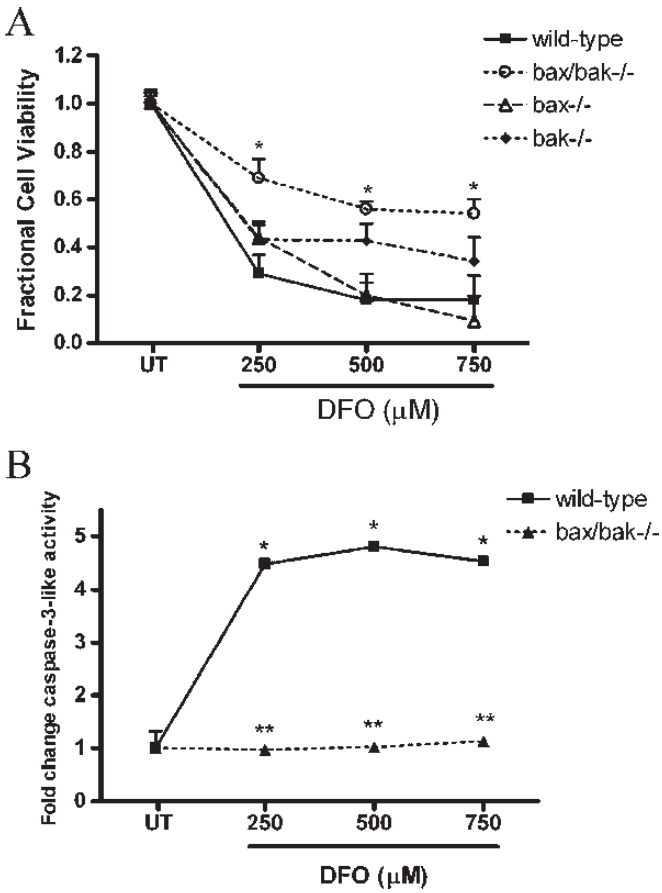

FIGURE 4. Loss of Bax and Bak attenuates desferrioxamine (DFO)-induced neural precursor cell (NPC) death and caspase-3 activation. **(A)** Bax/Bak-deficient NPCs exhibited significantly less death after 36 hours of exposure to DFO (250–750 μmol/L) compared with wild-type, $bax^{-/-}$, or $bak^{-/-}$ NPCs. *, $p < 0.01$ by 2-way analysis of variance (ANOVA)/Bonferroni post hoc test compared with both the wild-type and the knockout treated group. **(B)** Wild-type or Bax/Bak-deficient NPCs were treated with 250, 500, or 750 μmol/L DFO or media alone for 24 hours. Bax/Bak-deficient NPCs exposed to DFO showed a significant decrease in caspase-3–like activity compared with wild-type NPCs. The data represent mean ± SEM, with n = 5. *, $p < 0.01$ by 2-way ANOVA/Bonferroni post hoc test compared with both the wild-type and the knockout treated group.

treated with DFO for 12 and 24 hours showed a significant increase in cleaved caspase-3 compared with the control and 6-hour-DFO time point (Fig. 2A). Similarly, treatment with 500 μmol/L $CoCl_2$ for 24 hours caused a significant increase in cleaved caspase-3 (Fig. 2A). To assess caspase-3–like enzymatic activity, C17.2 cells were treated with normal media or 250 μmol/L DFO for 6 to 48 hours, and caspase-3–like activity was determined via the DEVD-AMC cleavage assay. Desferrioxamine-treated C17.2 cells exhibited a significant increase in caspase-3–like enzymatic activity by 24 hours (Fig. 2B). Similarly, OGD led to a significant increase in DEVD-AMC cleavage after 12 hours' exposure (Fig. 2C).

Hypoxia has been shown previously to cause either apoptotic or nonapoptotic cell death in other in vitro cell models (19, 24). To test whether caspase activity was required for DFO- or $CoCl_2$-induced NPC death, we treated NPCs with DFO or $CoCl_2$ alone or in the presence of boc-asp-FMK, a broad caspase inhibitor. Neural precursor cells treated with hypoxia mimetics in conjunction with boc-asp-FMK exhibited significantly less cell death than did NPCs treated with DFO or $CoCl_2$ (Fig. 2D), indicating that at least 1 component of hypoxia-induced NPC death is caspase-dependent.

To test the hypothesis that DFO-induced apoptosis requires new protein synthesis, we treated C17.2 cells with DFO alone or in the presence of the protein synthesis inhibitor cycloheximide. Cytosine arabinoside (AraC) was used as a control (25). We previously showed that AraC produces p53-dependent, transcription-dependent caspase-3 activation in NPCs (25). C17.2 neural stem cells were treated with fresh media in the presence or absence of DFO (500 μmol/L) and/or cycloheximide for 12 hours. Cycloheximide significantly reduced DFO-induced caspase-3–like enzymatic activity,

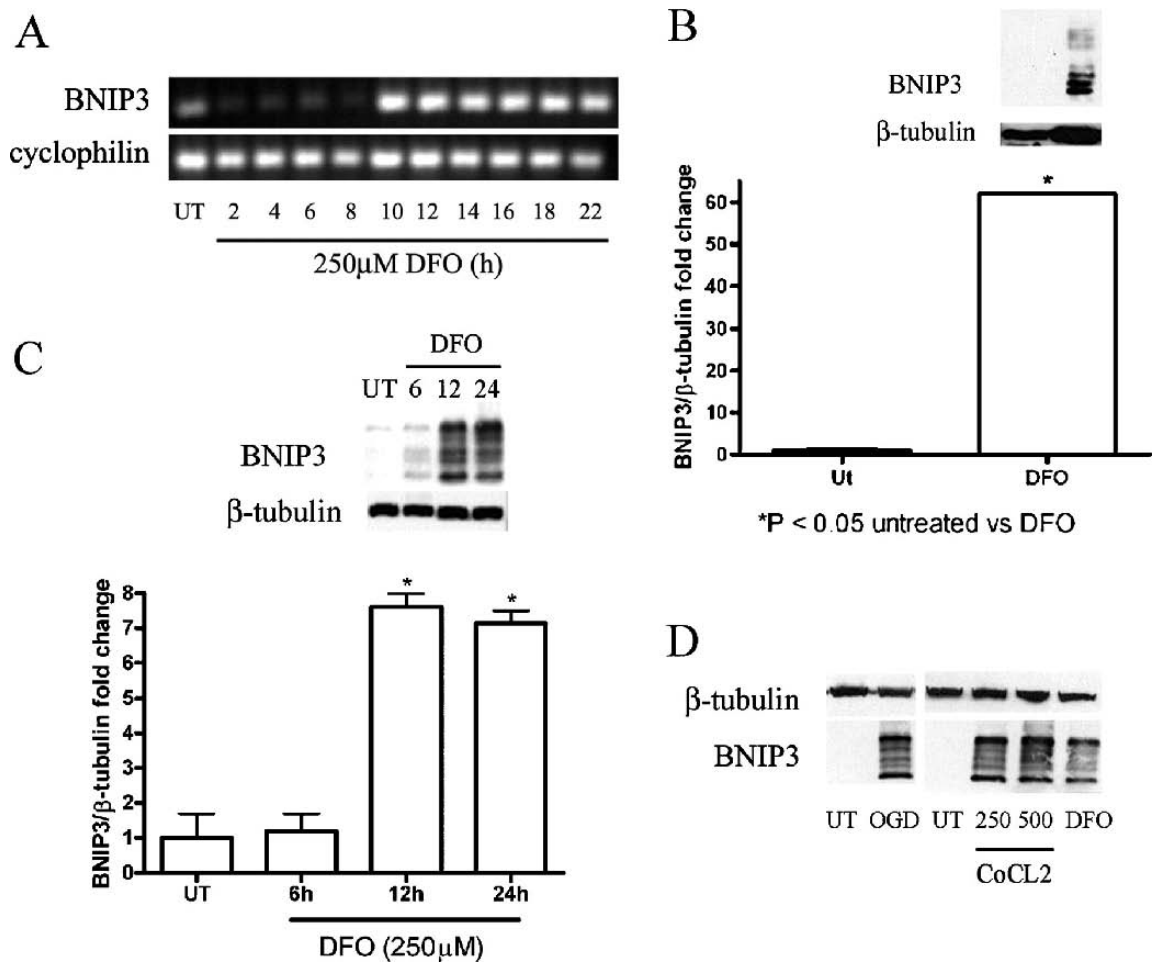

FIGURE 5. Hypoxia increases mRNA expression and protein levels of BNIP3. **(A)** An increase in BNIP3 mRNA expression was detected within 10 hours after desferrioxamine (DFO) (250 μmol/L) treatment and persisted for at least 10 hours compared with untreated (UT) cells and at 2- to 8-hour time points. Cyclophilin was used as a cDNA loading control. **(B)** Lysates from fibroblast growth factor-expanded neural precursor cells treated with 500 μmol/L DFO for 24 hours had significantly increased BNIP3 protein levels compared with UT cells. **(C)** C17.2 cells showed a time-dependent increase in BNIP3 protein levels after DFO exposure. Western blots for panels **B** and **C** were digitized by UN-SCAN-IT software, and averages for BNIP3/β-tubulin pixel totals were calculated and the data points expressed in fold change. Data points in panels **B** and **C** represent mean ± SEM, with n = 4. *, $p < 0.01$ by 1-way analysis of variance/Bonferroni post hoc test versus UT controls. **(D)** C17.2 cells subjected to oxygen glucose deprivation, cobalt chloride ($CoCl_2$), or DFO had increased BNIP3 levels relative to UT controls.

indicating that, like AraC-induced caspase activation, hypoxia-induced caspase-3 activation requires new protein synthesis (Fig. 2E).

Hypoxia Mimetics Cause an Increase in HIF-1α Expression and Protein Levels

Hypoxia mimetics have been shown to prevent ubiquitination and degradation of HIF-1α, leading to its dimerization with HIF-1β and induction of HIF-inducible genes (3, 6, 8). We hypothesized that hypoxia-induced NPC death and caspase activation resulted from decreased HIF-1α breakdown and increased HIF-1α transcriptional activity. To determine whether hypoxia mimetics lead to an increase in HIF-1α protein, C17.2 cells were treated with 250 μmol/L DFO or 500 μmol/L $CoCl_2$ for 24 hours followed by nuclear and nonnuclear fractionation. To confirm nonnuclear lysates, the mitochondria marker PDH was used, and to confirm nuclear lysates, the nuclear protein PARP was used. C17.2 cells treated with DFO had a significant increase in HIF-1α in nuclear fractions relative to controls (Figs. 3A, B).

Like hypoxia, DFO has been shown to cause HIF-1α stabilization, allowing it to dimerize with HIF-1β, leading to the activation of HIF-1α–inducible genes. Hypoxia-inducible factor 1α–regulated processes are dependent on transactivation of HIF-inducible genes and new protein synthesis. To determine whether DFO caused an increase in HIF-1α mRNA levels in NPCs, RT-PCR was performed on C17.2 cells treated with DFO compared with untreated controls. Hypoxia-inducible factor 1α gene expression was dramatically increased at 10 hours and remained elevated through 22 hours compared with untreated controls and earlier time points (Fig. 3C).

Hypoxia-Induced Death Requires Bax and Bak

To define the regulators of hypoxia-induced NPC death further, we investigated the proapoptotic Bcl-2 family members Bax and Bak. We have previously reported that Bax is a critical regulator of staurosporine- and DNA damage–induced NPC apoptosis (21, 25). To determine whether Bax/Bak deficiency inhibits DFO-induced death, wild-type, Bax-deficient, Bak-deficient, and Bax/Bak dual-deficient FGF2-expanded NPCs were treated with DFO for 24 hours. Bax/Bak-deficient NPCs were significantly protected from DFO-induced NPC death compared with wild-type NPCs or NPCs deficient in Bax or Bak alone (Fig. 4A). Wild-type and Bax/Bak-deficient NPCs were treated with 250, 500, and 750 μmol/L DFO for 24 hours, and caspase-3–like activity was measured via the DEVD-AMC cleavage assay. In

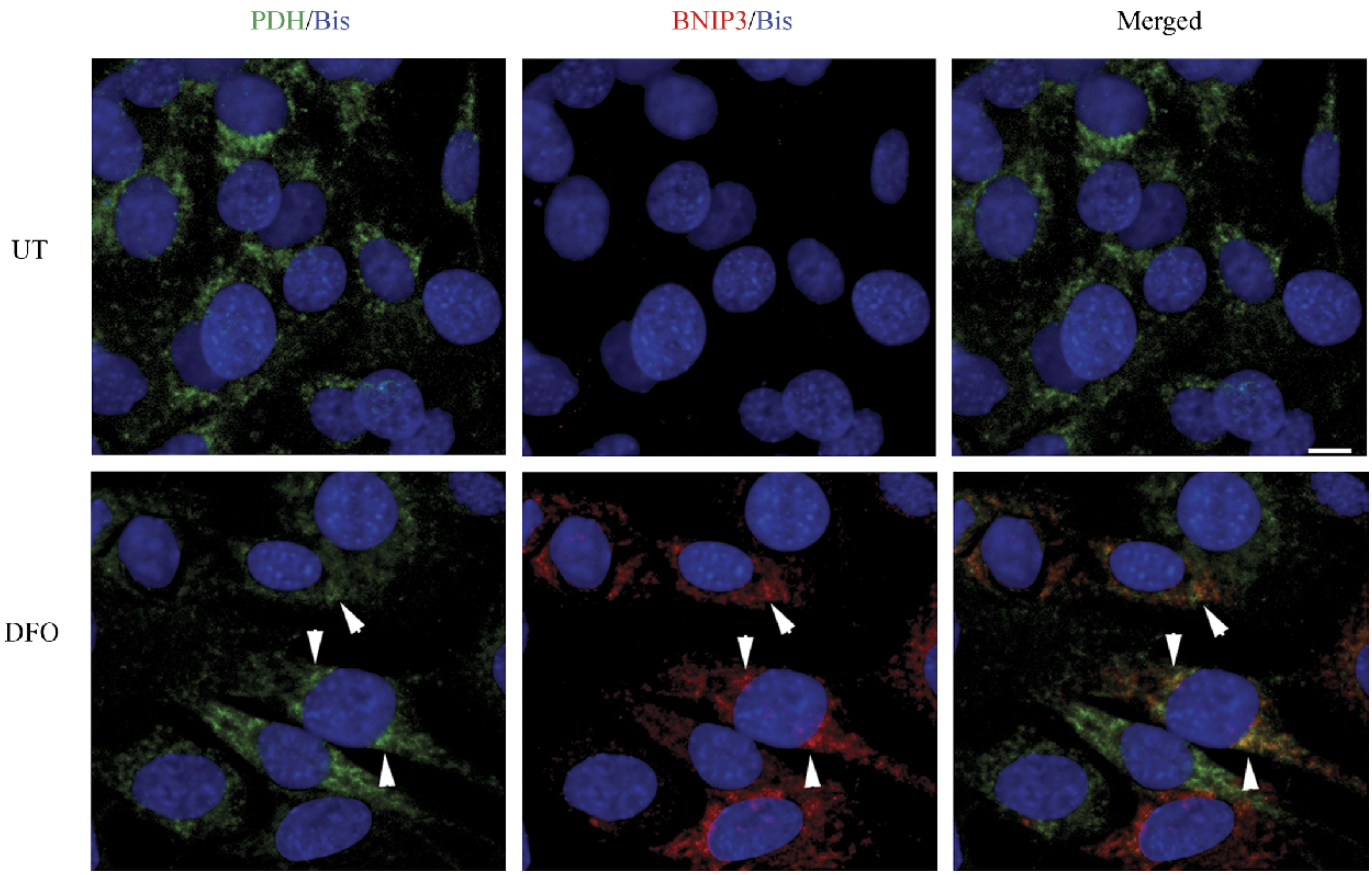

FIGURE 6. BNIP3 localizes to mitochondria after desferrioxamine (DFO) exposure. C17.2 cells were treated with 250 μmol/L DFO for 12 hours, fixed with 4% paraformaldehyde, and immunocytochemical detection of BNIP3 (red), pyruvate dehydrogenase (PDH, green), and bisbenzimide (Bis, blue) was performed. Confocal analysis revealed partial BNIP3 and PDH colocalization (arrowheads) after DFO exposure compared with untreated (UT) cells. Scale bar = 10 μm.

contrast to a robust increase in wild-type treated NPCs, Bax/Bak-deficient NPCs failed to show a significant increase in caspase-3–like activity after DFO (Fig. 4B). These data suggest a prominent role for Bax and Bak and the intrinsic mitochondrial apoptotic death pathway in regulating hypoxia-induced NPC death.

Upregulation of BNIP3 in Response to Hypoxia

BNIP3 is a known HIF-inducible gene and has been previously implicated in both cell death and autophagy regulation (13, 24). BNIP3 is a BH3-only Bcl-2 family member and has been previously reported to mediate cell death independent of Apaf1, caspase activation, and cytochrome C release (14, 26). BNIP3 mRNA levels were assessed to determine whether DFO caused an increase in BNIP3 transcription. RNA was extracted from C17.2 cells treated with DFO for 0 to 22 hours followed by cDNA synthesis. Reverse transcriptase–PCR revealed that BNIP3 expression was increased from 10 to 22 hours after DFO treatment compared with untreated controls and other time points (Fig. 5A). To examine the effects of hypoxia on BNIP3 protein levels, Western blot analysis was performed on

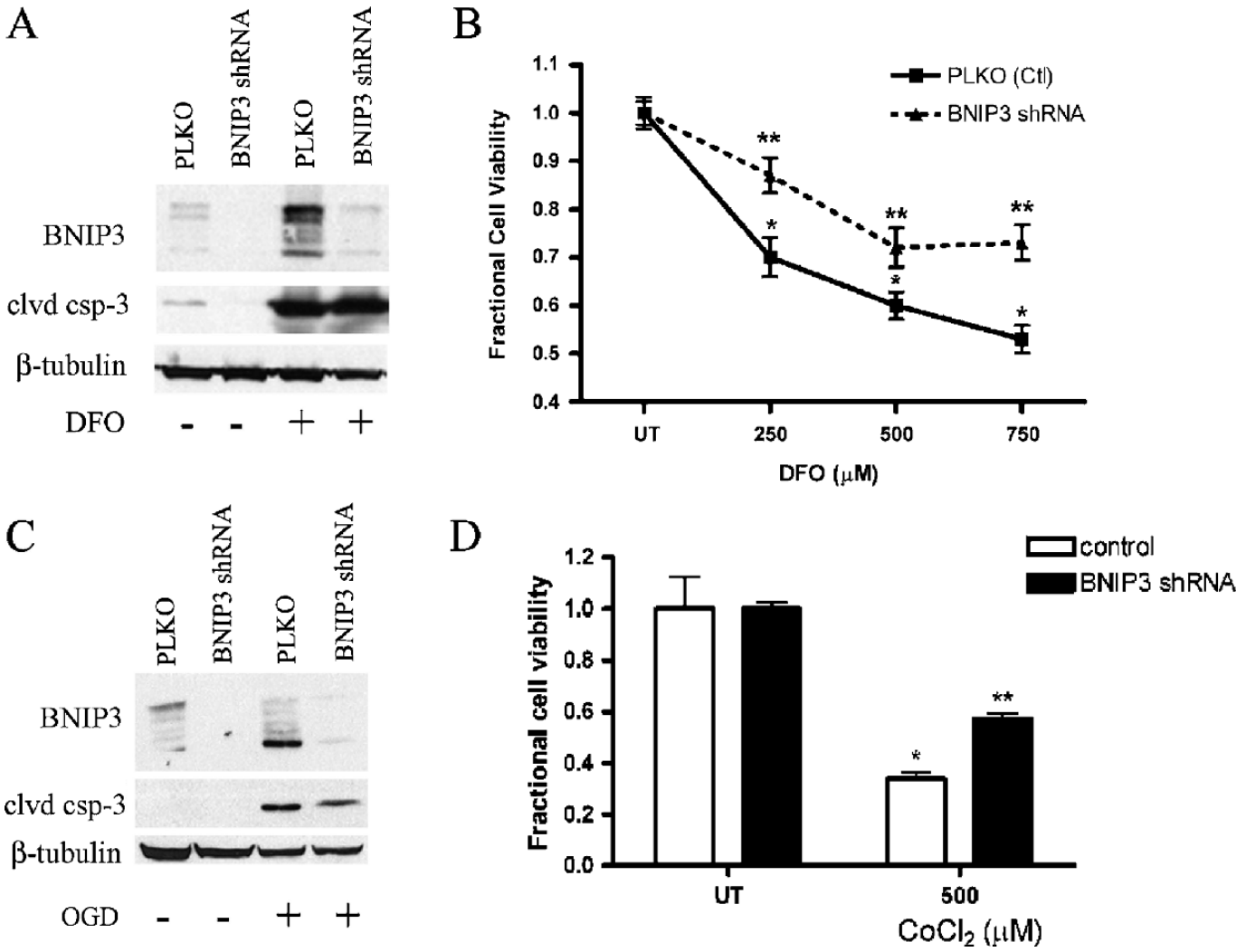

FIGURE 7. Knockdown of BNIP3 protects against hypoxia-induced death. **(A)** C17.2 cells infected with a lentivirus containing BNIP3 shRNA caused a decrease in BNIP3 protein levels compared with the empty vector control (PLKO). Western blot analysis with BNIP3 and β-tubulin as the loading control was performed after desferrioxamine (DFO) treatment for 24 hours. Lysates from DFO-treated BNIP3 shRNA cells exhibited robust cleaved caspase-3 protein (clvd csp-3) levels similar to lysates from control-treated cells. **(B)** C17.2 cells transduced with BNIP3 shRNA exhibited significantly attenuated DFO-induced death at concentrations between 250 and 750 μmol/L compared with the empty vector control. **(C)** Whole cell lysates from C17.2 cells containing BNIP3 shRNA or PLKO were subjected to oxygen glucose deprivation (OGD) and BNIP3, and cleaved caspase-3 protein levels were assessed. BNIP3 knockdown attenuated OGD-induced BNIP3 accumulation but not cleaved caspase-3. **(D)** C17.2 cells transduced with BNIP3 shRNA significantly attenuated cobalt chloride ($CoCl_2$)–induced death at 500 μmol/L compared with empty vector-treated cells. Data points for panels **B** and **D** represent mean ± SEM, with n = 6. *, $p < 0.01$ by 2-way analysis of variance (ANOVA)/Bonferroni post hoc test versus both PLKO treated or **, $p < 0.01$ by 2-way ANOVA/Bonferroni post hoc test versus BNIP3 knockdown treated.

FGF2-expanded NPCs and C17.2 cells treated with DFO for 24 hours. The BNIP3 protein has a predicted molecular weight of 22 kd, but previous reports have indicated that it runs at multiple bands between 22 and 28 kd and seems to form a dimer that exists around 50 to 55 kd (17, 27, 28). BNIP3 protein levels were significantly increased in DFO-treated, FGF2-expanded NPCs at 24 hours compared with untreated wild-type controls (Fig. 5B). BNIP3 levels were also assessed at 6 to 24 hours after DFO exposure or at 24 hours after $CoCl_2$ exposure and compared with untreated cells. Lysates from C17.2 cells treated with DFO at 12 and 24 hours and $CoCl_2$ (24 hours) revealed significant increases in BNIP3 isoforms (22–28 kd) (Fig. 5C). Similar to DFO-treated NPCs, whole cell lysates from C17.2 cells exposed to OGD or $CoCl_2$ also exhibited robust levels of BNIP3 compared with untreated NPCs (Fig. 5D). It has been

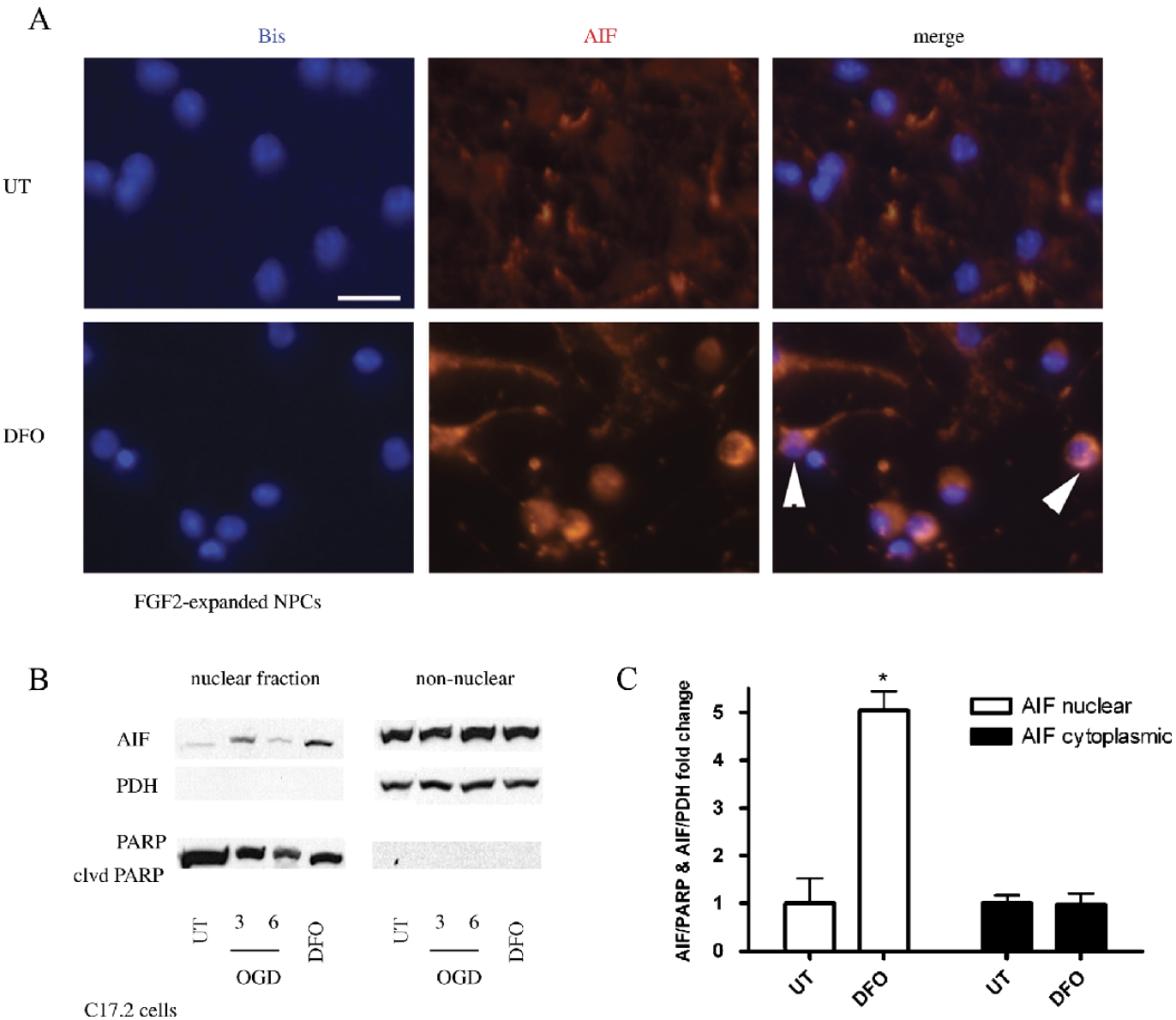

FIGURE 8. Hypoxia leads to increased nuclear AIF. **(A)** Fibroblast growth factor 2-expanded neural precursor cells were treated with 250 μmol/L desferrioxamine (DFO) for 24 hours, fixed with 4% paraformaldehyde, and immunostained for apoptosis-inducing factor (AIF) (red) and bisbenzimide (Bis) (blue). DFO exposure caused AIF translocation from the cytoplasm to the nucleus (white arrowheads). Scale bar = 20 μm. **(B)** C17.2 cells were subjected to oxygen glucose deprivation (OGD) (3–6 hours) and 250 μmol/L DFO (24 hours) followed by nuclear and cytoplasmic fractionation to assess AIF translocation to the nucleus. Western blot analysis revealed an increase in AIF levels in the nucleus after 3-hour OGD and 24-hour DFO treatment compared with untreated (UT) controls. Pyruvate dehydrogenase (PDH) was used as a cytoplasmic control and poly(ADP-ribose) polymerase (PARP) as a nuclear control. AIF/PARP or AIF/PDH pixel totals were calculated, and data points were expressed as fold change. Data points for **B** represent mean ± SEM, with n = 3. *, $p < 0.01$ by 1-way analysis of variance/Bonferroni post hoc test versus untreated controls. **(C)** AIF/PARP or AIF/PDH pixel totals were calculated, and data points were expressed as fold change.

reported that, upon activation, BNIP3 integrates into the mitochondria membrane to induce cell death. Dual-labeling immunocytochemistry and confocal analysis were performed to determine whether DFO treatment results in increased BNIP3 expression and mitochondria association. Consistent with the Western blot analysis, very little BNIP3 immunoreactivity was observed in untreated cells. Desferrioxamine-treated C17.2 cells exhibited markedly increased BNIP3 immunoreactivity that colocalized with the mitochondrial marker PDH (Fig. 6).

BNIP3 Regulates Hypoxia-Induced Neural Precursor Cell Death

To determine the role of BNIP3 in hypoxia-induced NPC death, we generated lentiviruses for shRNA targeting BNIP3. C17.2 cells and FGF2-expanded NPCs express only low levels of BNIP3. To assess BNIP3 knockdown, we treated C17.2 cells transduced with either a PLKO (Open Biosystems, Huntsville, AL) empty vector or BNIP3 shRNA with DFO or OGD and observed BNIP3 protein levels. BNIP3 protein levels were significantly decreased in C17.2 cells transduced with the BNIP3 shRNA compared with the untreated, DFO- and OGD-treated C17.2 cells (Figs. 7A, C). To investigate whether BNIP3 expression is important for hypoxia-induced NPC death, both PLKO control and BNIP3 shRNA-transduced C17.2 cells were plated and treated with DFO (250–750 μmol/L) or 500 μmol/L $CoCl_2$. BNIP3 knockdowns exhibited significant protection against DFO- and $CoCl_2$-induced NPC death compared with PLKO controls (Figs. 7B, D). Whole cell lysates were prepared from transduced cells treated with DFO for 24 hours or 6-hour OGD, and cleaved caspase-3 was assessed by Western blot

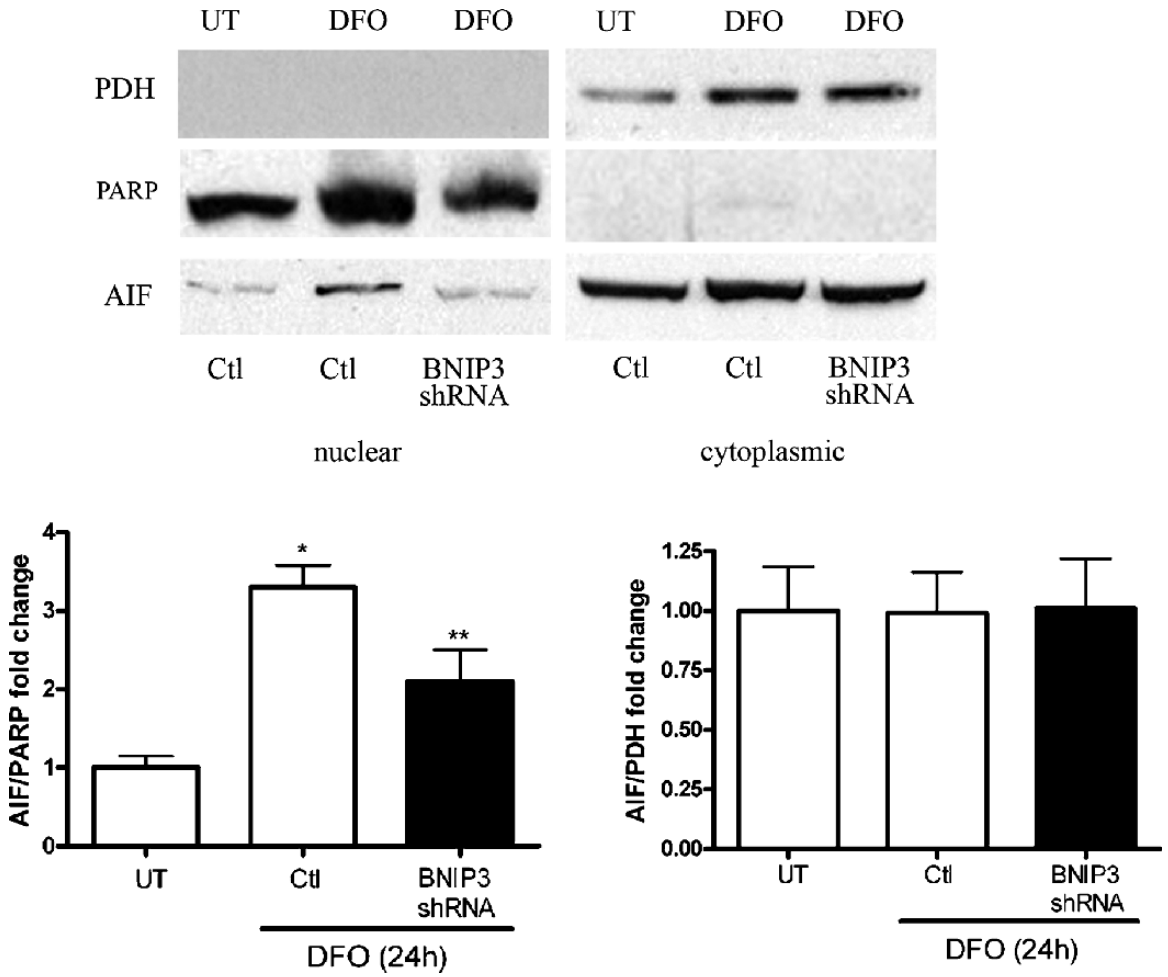

FIGURE 9. BNIP3 knockdown attenuates desferrioxamine (DFO)-induced apoptosis-inducing factor (AIF) translocation to the nucleus. Control C17.2 cells or BNIP3 knockdown cells were treated with 250 μmol/L DFO for 24 hours followed by nuclear and cytoplasmic fractionation. Western blot analysis for poly(ADP-ribose) polymerase (PARP) (nuclear marker), pyruvate dehydrogenase (PDH) (cytoplasmic marker), and AIF was performed. BNIP3 knockdown cells significantly attenuated DFO-induced AIF translocation from the mitochondria to the nucleus compared with control-treated cells. AIF levels in the cytoplasmic fraction remained unchanged between control and knockdown cells. AIF/PARP and AIF/PDH Western blots were scanned; pixel totals were calculated, and data points expressed as fold change. Data points represent mean ± SEM, with n = 3. *, $p < 0.01$ by 2-way analysis of variance (ANOVA)/Bonferroni post hoc test versus treated controls. **, $p < 0.01$ by 2-way ANOVA/Bonferroni post hoc test versus treated BNIP3 knockdowns.

analysis. Similar to previous reports using nonneuronal cells, DFO- and OGD-induced caspase activation was not prevented by BNIP3 knockdown (Figs. 7A, C) (29).

To investigate the potential mechanism of BNIP3-dependent, caspase-independent cell death in response to hypoxia, we performed immunocytochemical analysis for AIF after DFO treatment. Apoptosis-inducing factor regulates caspase-independent apoptosis in a variety of cell death models (30). Under normal conditions, AIF is localized to the mitochondria; however, previous studies have shown that hypoxia induces AIF translocation from the mitochondria to the nucleus to initiate cell death. Fibroblast growth factor 2–expanded NPCs treated with DFO for 24 hours showed both perinuclear and nuclear AIF localization in contrast to its mitochondrial localization in untreated cells (Fig. 8A). Western blot analysis performed on nuclear and cytoplasmic fractions from wild-type and 24-hour-DFO–treated C17.2 cells showed that C17.2 cells treated with DFO had a significant increase in AIF in the nuclear fraction compared with untreated controls (Fig. 8B). Apoptosis-inducing factor levels in the cytoplasmic fraction contained similar AIF levels in both wild-type controls and DFO-treated cells.

To explore the caspase-independent death pathway further, we tested the hypothesis that BNIP3 is important for AIF translocation from the mitochondria to the nucleus. C17.2 cells with either empty vector or BNIP3 shRNA were treated with DFO for 24 hours, and cytoplasmic and nuclear fractions were obtained. Western blot analysis revealed that AIF protein levels were significantly decreased in BNIP3 knockdown nuclear lysates compared with control-treated cells, whereas cytoplasmic AIF protein levels were unaltered (Fig. 9). These results suggest that, under hypoxic conditions, BNIP3 stimulates NPC death by promoting AIF release from the mitochondria.

DISCUSSION

Perinatal HI in humans is a frequent cause of cerebral palsy, and recent studies using rodent models of neonatal HI have shown that this stimulus causes significant NPC death (1, 31). In this study, we found that hypoxia mimetics and OGD activated both caspase-dependent and -independent NPC death pathways involving the Bcl-2 family members Bax, Bak, and BNIP3. Both OGD and hypoxia mimetics caused an increase in cleaved caspase-3 that was significantly reduced by Bax/Bak deficiency or protein synthesis inhibition. In addition, we found that both OGD and hypoxia mimetics increased BNIP3 and HIF-1α levels. By testing neural stem cells with BNIP3 knockdown, we showed that BNIP3 was involved in DFO- and OGD-induced death but not caspase activation. Desferrioxamine treatment also led to an increase in nuclear AIF, suggesting that BNIP3 causes HI-induced NPC death by localizing to the mitochondria and promoting AIF release and nuclear translocation. In total, our results indicate that hypoxia activates both the intrinsic apoptotic death pathway and a second caspase-independent death pathway involving BNIP3.

Although multiple transcription factors have been implicated in the regulation of hypoxia-induced death in various cell types, little is known about the upstream regulators of hypoxia-induced death in NPCs. Neural precursor cells exposed to hypoxia mimetics exhibited upregulation of HIF-1α mRNA and protein levels. Hypoxia-inducible factor 1α is an established regulator of BNIP3 that binds to the BNIP3 promoter; we found a significant increase in NPC BNIP3 protein levels after hypoxia (24). In a recent study, transglutaminase-2 attenuated OGD-induced BNIP3 activation by interacting with HIF-1β, thus preventing HIF-1α and β dimerization (23). Together with our results, these findings suggest that HIF-1α and HIF-1β promote hypoxia-induced NPC death and caspase activation via transcription of proapoptotic genes such as BNIP3.

Mitochondria membrane integration of proapoptotic Bcl-2 family members such as Bax and Bak induces mitochondrial dysfunction and plays an important role in caspase activation and cell death (14, 32). Our results revealed that DFO-induced caspase activation was virtually eliminated, and cell death was reduced significantly by dual Bax/Bak deficiency (Figs. 4A, B). Conversely, we identified the BH3-only proapoptotic protein, BNIP3, as an important mediator of DFO-induced NPC death, but not caspase activation. These results suggest that hypoxia activates both caspase-dependent and -independent death pathways in NPCs. Previous studies in cancer cells showed BNIP3-induced cell death by promoting Bax translocation to the mitochondria and activating Bax and Bak (33, 34). BNIP3 has been shown to interact with Bcl-2 and Bcl-XL, suggesting that BNIP3 can activate Bax and Bak via an indirect mechanism (35). Our studies revealed mitochondrial BNIP3 localization after hypoxia, but unlike Bax/Bak double-deficient NPCs, which showed minimal hypoxia-induced caspase-3 activation, BNIP3 was not required for caspase activation. These results indicate that BNIP3 is an important regulator of hypoxia-induced NPC death but not a critical regulator of Bax/Bak-dependent caspase activation in NPCs.

Our studies suggest that BNIP3 regulates DFO-induced caspase-independent NPC death by affecting the translocation of AIF from the mitochondria to the nucleus. Recent studies have shown that BNIP3-deficient mice subjected to myocardial ischemia/reperfusion have decreased infarct sizes compared with those of wild-type mice (36, 37). In addition, harlequin mice carrying an AIF mutation rendering it approximately 60% inactive contained smaller brain infarct volumes compared with wild-type mice after HI exposure (30, 38). Consistent with the results of our studies, the harlequin mutation did not prevent HI-induced cytochrome C release or caspase activation. These findings suggest that hypoxia initiates 2 parallel death pathways in vivo: one that involves a caspase-independent death that is regulated by AIF and BNIP3 and a second caspase-dependent signaling cascade involving Bax and Bak.

In total, our studies indicate that hypoxia causes activation of multiple prodeath pathways in NPCs. One such pathway involves the Bax/Bak-dependent intrinsic apoptotic death program and caspase-3 activation, whereas a second pathway consists of HIF-induced BNIP3 expression and subsequent AIF translocation from mitochondria to the nucleus to trigger caspase-independent cell death. These findings illustrate the dynamic interplay between cell death

pathways and further highlight the stimulus-specific nature of NPC death regulation.

ACKNOWLEDGMENTS

The authors thank UAB Neuroscience Core Facilities (NS47466 and NS57098) and the UAB Civitan International Research Center (K.C.W.) for additional support. They also thank Shawn Williams and Ms Cecelia Latham for technical assistance, Ms Angela Schmeckebier for manuscript preparation, and Dr John Shacka for critical review of the manuscript.

REFERENCES

1. Romanko MJ, Zhu C, Bahr BA, et al. Death effector activation in the subventricular zone subsequent to perinatal hypoxia/ischemia. J Neurochem 2007;103:1121–31
2. An WG, Kanekal M, Simon MC, et al. Stabilization of wild-type p53 by hypoxia-inducible factor 1alpha. Nature 1998;392:405–8
3. Epstein AC, Gleadle JM, McNeill LA, et al. *C. elegans* EGL-9 and mammalian homologs define a family of dioxygenases that regulate HIF by prolyl hydroxylation. Cell 2001;107:43–54
4. Jaakkola P, Mole DR, Tian YM, et al. Targeting of HIF-alpha to the von Hippel-Lindau ubiquitylation complex by O_2-regulated prolyl hydroxylation. Science 2001;292:468–72
5. Ivan M, Kondo K, Yang H, et al. HIF-α targeted for VHL-mediated destruction by proline hydroxylation: Implications for O_2 sensing. Science 2001;292:464–68
6. Berra E, Roux D, Richard DE, et al. Hypoxia-inducible factor-1 alpha (HIF-1 alpha) escapes O(2)-driven proteasomal degradation irrespective of its subcellular localization: Nucleus or cytoplasm. EMBO Rep 2001;2:615–20
7. Richard DE, Berra E, Gothie E, et al. p42/p44 mitogen-activated protein kinases phosphorylate hypoxia-inducible factor 1alpha (HIF-1α) and enhance the transcriptional activity of HIF-1. J Biol Chem 1999;274:32631–37
8. Berra E, Richard DE, Gothie E, et al. HIF-1-dependent transcriptional activity is required for oxygen-mediated HIF-1α degradation. FEBS Lett 2001;491:85–90
9. Hirsila M, Koivunen P, Xu L, et al. Effect of desferrioxamine and metals on the hydroxylases in the oxygen sensing pathway. FASEB J 2005;19:1308–10
10. Guo M, Song LP, Jiang Y, et al. Hypoxia-mimetic agents desferrioxamine and cobalt chloride induce leukemic cell apoptosis through different hypoxia-inducible factor-1alpha independent mechanisms. Apoptosis 2006;11:67–77
11. Clarke PG. Developmental cell death: Morphological diversity and multiple mechanisms. Anat Embryol (Berl) 1990;181:195–213
12. Akhtar RS, Ness JM, Roth KA. Bcl-2 family regulation of neuronal development and neurodegeneration. Biochim Biophys Acta 2004;1644:189–203
13. Azad MB, Chen Y, Henson ES, et al. Hypoxia induces autophagic cell death in apoptosis-competent cells through a mechanism involving BNIP3. Autophagy 2008;4:195–204
14. Vande VC, Cizeau J, Dubik D, et al. BNIP3 and genetic control of necrosis-like cell death through the mitochondrial permeability transition pore. Mol Cell Biol 2000;20:5454–68
15. Kanzawa T, Zhang L, Xiao L, et al. Arsenic trioxide induces autophagic cell death in malignant glioma cells by upregulation of mitochondrial cell death protein BNIP3. Oncogene 2005;24:980–91
16. Zhang L, Li L, Liu H, et al. HIF-1alpha activation by a redox-sensitive pathway mediates cyanide-induced BNIP3 upregulation and mitochondrial-dependent cell death. Free Radic Biol Med 2007;43:117–27
17. Daido S, Kanzawa T, Yamamoto A, et al. Pivotal role of the cell death factor BNIP3 in ceramide-induced autophagic cell death in malignant glioma cells. Cancer Res 2004;64:4286–93
18. Pattingre S, Tassa A, Qu X, et al. Bcl-2 antiapoptotic proteins inhibit Beclin 1–dependent autophagy. Cell 2005;122:927–39
19. Zhang H, Bosch-Marce M, Shimoda LA, et al. Mitochondrial autophagy is an HIF-1-dependent adaptive metabolic response to hypoxia. J Biol Chem 2008;283:10892–903
20. Knudson CM, Tung KS, Tourtellotte WG, et al. Bax-deficient mice with lymphoid hyperplasia and male germ cell death. Science 1995;270:96–99
21. Geng Y, Akhtar RS, Shacka JJ, et al. p53 transcription-dependent and -independent regulation of cerebellar neural precursor cell apoptosis. J Neuropathol Exp Neurol 2007;66:66–74
22. Snyder EY, Deitcher DL, Walsh C, et al. Multipotent neural cell lines can engraft and participate in development of mouse cerebellum. Cell 1992;68:33–51
23. Filiano AJ, Bailey CD, Tucholski J, et al. Transglutaminase 2 protects against ischemic insult, interacts with HIF1β, and attenuates HIF1 signaling. FASEB J 2008;22:2662–75
24. Tracy K, Dibling BC, Spike BT, et al. BNIP3 is an RB/E2F target gene required for hypoxia-induced autophagy. Mol Cell Biol 2007;27:6229–42
25. Akhtar RS, Geng Y, Klocke BJ, et al. Neural precursor cells possess multiple p53-dependent apoptotic pathways. Cell Death Differ 2006;13:1727–39
26. Chen G, Cizeau J, Vande VC, et al. Nix and Nip3 form a subfamily of pro-apoptotic mitochondrial proteins. J Biol Chem 1999;274:7–10
27. Fei P, Wang W, Kim SH, et al. Bnip3L is induced by p53 under hypoxia, and its knockdown promotes tumor growth. Cancer Cell 2004;6:597–609
28. Zhang Z, Yang X, Zhang S, et al. BNIP3 upregulation and EndoG translocation in delayed neuronal death in stroke and in hypoxia. Stroke 2007;38:1606–13
29. Tracy K, Macleod KF. Regulation of mitochondrial integrity, autophagy and cell survival by BNIP3. Autophagy 2007;3:616–19
30. Zhu C, Wang X, Huang Z, et al. Apoptosis-inducing factor is a major contributor to neuronal loss induced by neonatal cerebral hypoxia-ischemia. Cell Death Differ 2007;14:775–84
31. Brazel CY, Nunez JL, Yang Z, et al. Glutamate enhances survival and proliferation of neural progenitors derived from the subventricular zone. Neuroscience 2005;131:55–65
32. Chipuk JE, Kuwana T, Bouchier-Hayes L, et al. Direct activation of Bax by p53 mediates mitochondrial membrane permeabilization and apoptosis. Science 2004;303:1010–14
33. Kubli DA, Quinsay MN, Huang C, et al. Bnip3 functions as a mitochondrial sensor of oxidative stress during myocardial ischemia and reperfusion. Am J Physiol Heart Circ Physiol 2008;295:H2025–31
34. Kubli DA, Ycaza JE, Gustafsson AB. Bnip3 mediates mitochondrial dysfunction and cell death through Bax and Bak. Biochem J 2007;405:407–15
35. Ray R, Chen G, Vande VC, et al. BNIP3 heterodimerizes with Bcl-2/Bcl-X(L) and induces cell death independent of a Bcl-2 homology 3 (BH3) domain at both mitochondrial and nonmitochondrial sites. J Biol Chem 2000;275:1439–48
36. Diwan A, Krenz M, Syed FM, et al. Inhibition of ischemic cardiomyocyte apoptosis through targeted ablation of Bnip3 restrains postinfarction remodeling in mice. J Clin Invest 2007;117:2825–33
37. Hochhauser E, Cheporko Y, Yasovich N, et al. Bax deficiency reduces infarct size and improves long-term function after myocardial infarction. Cell Biochem Biophys 2007;47:11–20
38. Zhu C, Wang X, Deinum J, et al. Cyclophilin A participates in the nuclear translocation of apoptosis-inducing factor in neurons after cerebral hypoxia-ischemia. J Exp Med 2007;204:1741–48